Preparation and Porosity Characterization of Highly Cross-Linked Polymer Resins Derived from Multifunctional (Meth)acrylate Monomers

T. Rohr,[†] S. Knaus,[†] H. Gruber,[†] and D. C. Sherrington*[,‡]

Chemical Technology of Organic Materials, Vienna University of Technology, Getreidemarkt 9/162, 1060 Vienna, Austria, and Department of Pure & Applied Chemistry, University of Strathclyde, 295 Cathedral Street, Glasgow G1 1XL, U.K.

Received June 25, 2001; Revised Manuscript Received October 11, 2001

ABSTRACT: Permanently porous polymer resins derived from multifunctional (meth)acrylate monomers have been prepared by suspension polymerization. The dry state porosity characteristics have been evaluated using N_2 sorption and Hg intrusion porosimetry, and the results correlated in terms of the three-dimensional cohesion parameter, δ_t, of the polymers and porogens. The pore size distributions of almost all resins cover a broad range from micro- through meso- to macropores. The porosity data had to be computed from the adsorption branches of the N_2 sorption isotherms, since an artifact arises in the pore size distributions if derived from the corresponding desorption data. The artifact is attributed to a percolation process in the desorption mechanism. The correlation of porosity data (e.g., the Brunauer, Emmett, and Teller (BET) surface area and the Barret, Joyner, and Halenda (BJH) average pore radius) with the nature of the porogen was found to be very limited if the one-dimensional Hildebrand solubility parameter, δ, only is used. However, by application of a group contribution method due to Hoftyzer−Van Krevelen and Hoy, three-dimensional cohesion parameters, δ_t, and the porogen−polymer affinity parameters, d_0, could be calculated. Using the latter as the basis for a new correlation the N_2 sorption BET computed surface areas of resins show an inverse proportional relationship with d_0, while BJH average pore radii show a proportional relationship.

Introduction

The use of gel type and permanently porous resins based upon styrene or methacrylate monomers, and also polysaccharide-derived species, continues to rise. Exploitation occurs in areas a diverse as chromatography,[1] solid-phase combinatorial and parallel synthesis,[2,3] polymer-supported catalysts,[4] primary and secondary metal ion recovery, surface and groundwater purification,[5] and downstream treatment of organic chemical streams, and biochemical aqueous streams.[6] For many applications it is important to utilize a porous resin with a high surface area, and while methodologies exist for producing such materials, understanding, predicting, and fine-tuning the porosity characteristics of resins remain problematical.

Multifunctional (meth)acrylate monomers offer a convenient and cost-effective route to porous resins. Several groups have described the preparation and characterization of cross-linked polymers derived from multifunctional (meth)acrylates employing either solution or suspension polymerization methods. The porous structures of homo- and copolymers of trimethylolpropane trimethacrylate (TRIM) were investigated by Flodin et al.[7−12] and Viklund et al.,[13] and similar studies of homo- and copolymers of trimethylolpropane triacrylate[14−17] and other multifunctional (meth)acrylates[18] have been reported by Kolarz and co-workers and indeed others.[19] Recently, polymer resins from TRIM have been synthesized by sol−gel and suspension polymerization using supercritical CO_2 as the porogen.[20,21]

In the present paper we report on our synthesis by suspension polymerization of porous homopolymers of TRIM, pentaerythritol triacrylate (PETrA), pentaerythritol tetraacrylate (PETeA), and dipentaerythritol penta-/hexaacrylate (DPEHA) produced using a range of porogens. The dry state porosity characteristics have been evaluated using N_2 sorption and Hg intrusion porosimetry, and the results correlated in terms of the three-dimensional cohesion parameter, δ_t,[22−24] of the polymers and porogens.

In the literature describing ion-exchange resins, the terms "macroporosity" and "macroporous" are often used as synonyms for porosity in general. In this paper, however, we will restrict our use of the terms micropores, mesopores, and macropores to the definitions recommended by IUPAC,[25] i.e., micropores, pore widths <2 nm; mesopores, pore widths 2−50 nm; and macropores, pore widths >50 nm. When referring more loosely to a porous structure, we will use the expression "permanently porous" as opposed to "macroporous".

Experimental Section

Materials. Dipentaerythritol penta-/hexaacrylate (DPEHA), pentaerythritol triacrylate (PETrA, tech.), pentaerythritol tetraacrylate (PETeA), trimethylolpropane trimethacrylate (TRIM), butyl acetate (99+%), ethyl isobutyrate (99%), isobutyl acetate (99%), propyl acetate (99%), 2-aminoethyl methacrylate hydrochloride, and potassium ferricyanide(III) were obtained from Aldrich Chemical Co. Ltd. Potassium bromide was obtained from Fluka, and benzoyl peroxide (75%) was obtained from Merck Ltd. Hydroxyethyl cellulose (Tylose H 10000) was obtained as a gift from Hoechst AG. All chemicals were used without further purification.

Instrumentation. N_2 sorption isotherms were generated using a Micromeritics ASAP 2010 instrument. Samples were dried at 100 °C for at least 6 h at high vacuum before sorption was initiated. BET surface areas, BJH pore size distributions, and micropore distributions (Dubinin-Astakhov) were computed using the Micromeritics software package associated with the instrument. In the case of the BJH pore distributions the data derived from the adsorption branch of each isotherm

[†] Vienna University of Technology.
[‡] University of Strathclyde.

10.1021/ma0110958 CCC: $22.00
Published on Web 11/29/2001

Table 1. Experimental Conditions and Porosity Measurements for Resins 1−21

						N_2 adsorption			
resin	monomer	porogen[a]	monomer: porogen [g/g]	yield 106−425 μm [%]	double bond content [%]	BET area [$m^2\ g^{-1}$]	*C* value	pore vol[b] [$cm^3\ g^{-1}$]	BJH av *R* [μm]
1	TRIM	BA	1:4	67.3	13.0	425	89	0.66 (0.56)	0.0038
2	TRIM	BA	1:2	95.0	11.0	579	108	1.11 (1.11)	0.0049
3	TRIM	BA	1:1	90.7	11.5	557	116	0.68 (0.55)	0.0029
4	TRIM	BA	3:2	94.2	9.5	504	150	0.33 (0.17)	0.0020
5	TRIM	BA	2:1	94.0	11.5	375	245	0.14 (0.09)	0.0016
6	TRIM	PA	1:4	90.4	11.5	538	119	0.95 (1.27)	0.0047
7	TRIM	PA	1:2	95.7	10.5	606	115	0.87 (0.54)	0.0038
8	TRIM	PA	2:3	88.7	11.5	589	118	0.64 (0.33)	0.0030
9	TRIM	PA	1:1	92.6	8.5	530	158	0.31 (0.32)	0.0019
10	TRIM	EIB	1:1	98.0	13.5	554	113	0.61 (0.56)	0.0029
11	TRIM	IBA	1:1	96.8	11.0	591	126	0.57 (0.51)	0.0027
12	TRIM	X	1:1	95.2	15.0	436	93	0.51 (0.50)	0.0029
13	PETrA	BA	1:1	96.6	15.5	471	89	0.70 (0.69)	0.0035
14	PETrA	X	1:1	87.3	23.5	228	61	0.57 (0.77)	0.0050
15	PETeA	BA	1:1	86.6	11.0	556	107	0.84 (0.79)	0.0036
16	PETeA	X	1:1	93.0	14.5	261	67	0.59 (0.82)	0.0047
17	DPEHA	BA	1:1	97.1	13.0	607	111	0.77 (0.71)	0.0031
18	DPEHA	PA	1:1	97.6	16.5	336	121	0.17 (0.21)	0.0016
19	DPEHA	EIB	1:1	97.0	22.0	584	120	0.72 (0.30)	0.0032
20	DPEHA	IBA	1:1	99.5	24.5	595	114	0.72 (0.63)	0.0031
21	DPEHA	X	1:1	96.3	24.0	318	66	0.67 (0.82)	0.0043

[a] X (xylene), BA (butyl acetate), EIB (ethyl isobutyrate), IBA (isobutyl acetate), PA (propyl acetate). [b] Data for the pore volume derived from mercury intrusion experiments are put in parentheses.

was regarded as the more definitive (see Discussion section). Mercury intrusion porosimetry was carried out using a Micromeritics Autopore II 9220 instrument, and the data were manipulated with the custom software. IR spectra were recorded on a Bio-Rad FTS 135 spectrometer.

Resin Synthesis. Resin beads were prepared by suspension polymerization. Typically the aqueous phase (650 g) comprised 0.16% (1.04 g) of hydroxyethyl cellulose and the organic phase (50 g overall mass) was of the compositions shown in Table 1. Benzoyl peroxide (1 wt % relative to monomer) was dissolved in the porogen, the solution added to the monomer, and the mixture purged with N_2 for 5 min. The aqueous phase was added to a 1000 mL parallel-sided flanged gastight glass vessel fitted with a metal stirrer carrying two impellers. The solution was purged with N_2 for 10 min, and then the organic phase was added, leaving a slow N_2 flow. The stirrer speed was set to 420 rpm, and the polymerization was allowed to proceed at 80 °C for 8 h. The beads were filtered using a 75 μm sieve, washed with aqueous methanol (30%, 1000 mL) extracted with acetone in a Soxhlet apparatus for 24 h, and then vacuum-dried at 40° C for 24 h. The resulting beads were then size fractionated using sieves, and the fraction between 106 and 425 μm was used in all experiments (see Table 1 for yields).

Determination of Residual Double Bond Content in Resins. For each resin a powdered sample mixture containing polymer (10 mg) and reference standard, potassium ferricyanide (10 mg), and potassium bromide (480 mg) was prepared. A calibrant mixture was also prepared containing 2-aminoethyl methacrylate hydrochloride (10 mg) and potassium bromide (2000 mg). KBr disks were prepared containing a portion of the sample mixture (50 mg) and various levels of the calibrant mixture (0, 25, 50, and 100 mg) and additional KBr to make up a fixed overall mass of 200 mg. The characteristic band for the C═C double bond at 810 cm^{-1} was normalized against the band from the reference standard at 2100 cm^{-1}. The residual C═C double bond content in each sample was calculated from the intensity data from the KBr disks containing known levels (0 → upward) of the calibrant using an appropriate curve-fitting routine.

Results and Discussion

Preparation of Resins. Polymer resins **1**−**21** were prepared by a standardized suspension polymerization procedure as indicated in the Experimental Section. The aqueous phase (650 g) contained 0.16 wt % hydroxyethylcellulose as a stabilizer, and the overall mass of the organic phase was always 50 g. The compositions of each polymerization mixture are indicated in Table 1. The ratio of monomer:porogen (g/g) was varied between 1:4 and 2:1 in the case of TRIM with butyl acetate as the porogen, resins **1**−**5**, and between 1:4 and 1:1 when propyl acetate was used, resins **6**−**9**. All other resins were prepared with a monomer:porogen ratio of 1:1 irrespective of the multifunctional (meth)acrylate monomer or porogen employed. Once the polymerization conditions detailed in the Experimental Section were established, high-quality resin beads in the size range 106−425 μm were obtained consistently in high or very high yields, confirming the effectiveness of hydroxyethylcellulose as a robust stabilizer for these (meth)acrylate suspension polymerizations.

Since the real level of cross-linking is known to be an important parameter in the generation of the porous morphology of resins,[26,28] contributing substantially to controlling the point of phase separation of the growing polymer matrix from the porogen, it was thought important to assess the level of unreacted C═C bonds in the resins and in particular to assess how consistent this figure was. Attempts to do this by reacting the resins with Br_2 followed by elemental microanalysis of the modified polymers gave erratic and inconsistent results. Consequently, the rather unusual FTIR spectroscopic method detailed in the Experimental Section was evolved in which the intensity of the characteristic C═C stretching band at 810 cm^{-1} was measured normalized against the intensity of a standard reference band at 2100 cm^{-1}. Calibration was achieved using known levels of 2-aminoethyl methacrylate hydrochloride as the source of the C═C 810 cm^{-1} band. Although this procedure needed care and was rather tedious, in fact the procedure proved to be more reproducible than the Br_2 addition procedure, and the error in the data in Table 1 is ∼±5%. From these data it is clear that in the case of the resins derived from TRIM, typically ∼11 ± 5% of the C═C bands remain unreacted. These figures are in the range of those reported earlier by Flodin et

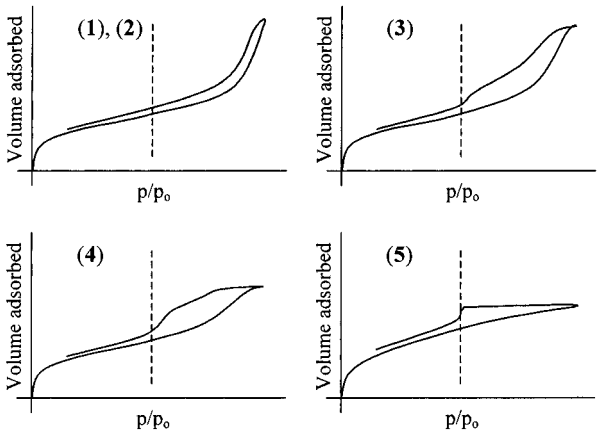

Figure 1. Qualitative representation of N_2 sorption isotherms and hysteresis loop shapes for TRIM resins **1**−**5** prepared in butyl acetate as porogen. Resins **1** and **2** represent type II isotherms and type H3 hysteresis loops, resins **3** and **4** represent types IV/H2, and resin **5** represents type I/H4.

al.[7,8] and perhaps somewhat surprisingly show no significant variation even when the monomer:porogen (butyl acetate) ratio (g/g) is varied from 1:4 to 2:1 (resins **1**−**5**). For example, it might have been expected that the high porogen content used in **1** might have allowed more efficient polymerization of the methacrylate groups in TRIM. However, this is not the case, and the controlling factor seems to be that each of the TRIM resins synthesized is in fact a homopolymerization of TRIM, effectively producing a common structural network within which the topographical relationship of unreacted pendant C=C bonds is presumably very similar. This is also even more likely to be the case when the polymer matrix phase separates from the porogen. The consistency of the residual C=C bond content within the TRIM resins allows the assumption that the real level of cross-linking in these species is very similar. It is possible that the number of permanent chain entanglements varies, but this is a parameter that is almost impossible to assess, and so the differences in morphology will be discussed in terms of the different level and nature only of the porogen employed.

The level of residual C=C bonds in the resins prepared from the other multifunctional acrylates (resins **13**−**21**, Table 1) is more variable, and hence the level of real cross-linking is also more variable. Overall, and perhaps not too surprising, as the multifunctionality of the monomer rises so the efficiency of polymerization of acrylate groups falls, and the level of residual C=C bonds rises. In the case of the penta/hexaacrylate, DPEHA, up to ∼25% of acrylate groups remain intact depending on the porogen employed.

Clearly in exploiting these resins the residual C=C bonds offer an opportunity for further chemical modification as reported by Hubbard et al.[29]

Surface Area and Pore Structure of TRIM Resins Employing Butyl and Propyl Acetates as Porogens. The pore structure of all resins was probed using N_2 sorption porosimetry and application of relevant modeling theories in order to generate pore size distribution, pore volume, and surface area data. Qualitative representations of the adsorption and desorption isotherms, indicating the hysteresis phenomena which arise, are shown in Figure 1 in the case of resins **1**−**5**. Resins **1** and **2** display an incomplete type II isotherm and a type H3 hysteresis loop; resins **3** and **4** show

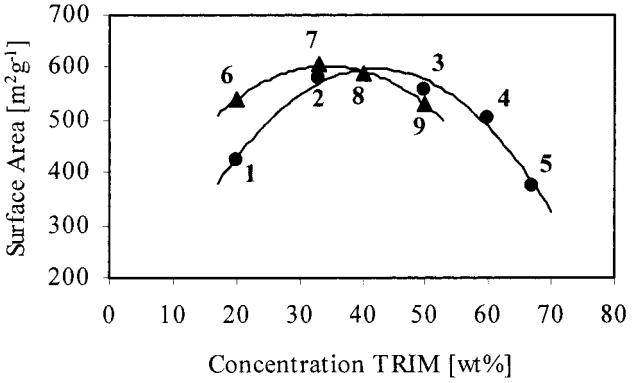

Figure 2. N_2 sorption BET surface area of TRIM resins prepared using butyl acetate, ● (**1**−**5**), and propyl acetate, ▲ (**6**−**9**), as porogens.

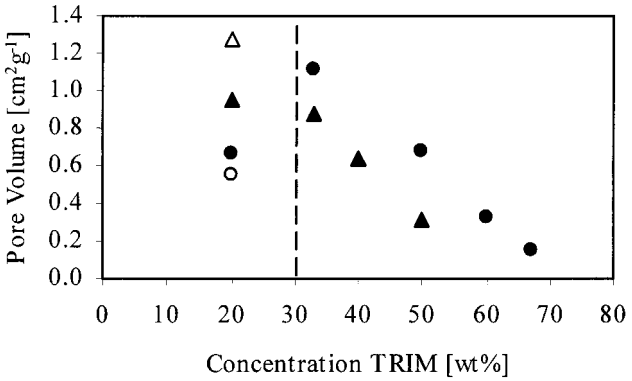

Figure 3. Pore volume of TRIM resins derived from N_2 sorption data: butyl acetate as porogen, ●, ○ (**1**−**5**); propyl acetate as porogen, ▲, △ (**6**−**9**). Open points refer to data derived from Hg intrusion measurements.

manifestations of a type IV isotherm and a type H2 hysteresis loop, while resin **5** can rather be associated with a type I isotherm and a type H4 hysteresis loop.[25,30]

Comparing the N_2 sorption Brunauer, Emmett, and Teller (BET) surface areas[31] of the TRIM resins **1**−**12** (Table 1) with the analogous data for the polymer gels described by Flodin et al.,[7−12] very similar values, 300−600 $m^2\ g^{-1}$, are apparent. The Swedish group reported that changes in the pore structure led in some cases to linear, but in others to nonlinear, relationships between the surface area and the concentration of monomer in the porogen.[7,8] The BET surface area and corresponding pore volume as a function of monomer concentration in the porogen for our TRIM resins are shown in Figures 2 and 3, respectively. A maximum in the BET surface area is seen ∼30 wt % TRIM in propyl acetate and ∼40 wt % in butyl acetate (Figure 2). The data show good fits to second-order polynomials (solid lines). In contrast, the corresponding pore volumes show an almost linear increase with decreasing monomer concentration (Figure 3), in keeping with the larger volume of porogen present as the monomer content is reduced. There is, however, an apparent drop in pore volume below ∼30 wt % TRIM (dotted line, Figure 3) which might be indicative of collapse of the pore structure in resins **1** and **6** on drying. The polymer matrix formed below 30 wt % TRIM might simply be too expanded and mechanically fragile to survive completely intact on drying. Whether this collapse is reversible or not on reswelling in a thermodynamically good solvent is not clear from the limited data to hand, but such reversibly collapsible porous styrene−divinylbenzene resins have been char-

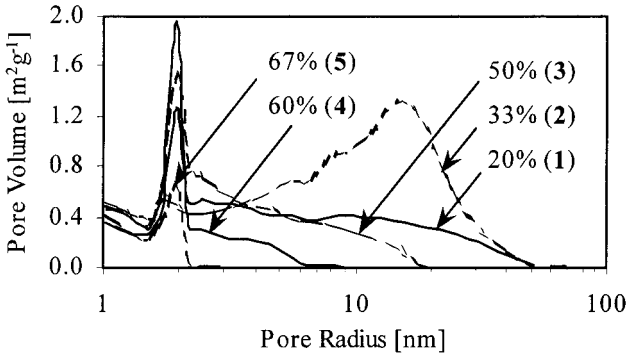

Figure 4. N_2 sorption BJH pore size distribution of TRIM resins **1**−**5** calculated from desorption branches of the isotherms.

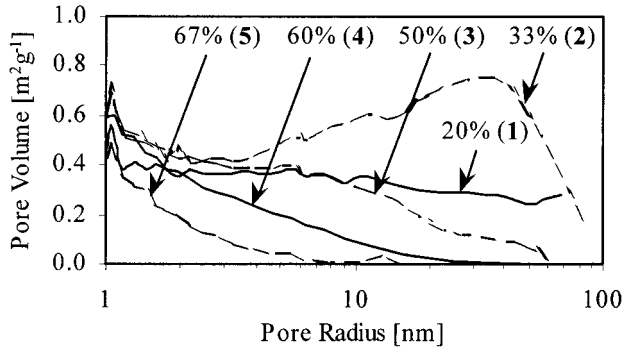

Figure 5. N_2 sorption BJH pore size distribution of TRIM resins **1**−**5** calculated from adsorption branches of the isotherms.

acterized by Sherrington and his collaborators[32] and by Hradil and Svec.[33] It is however important to realize that resins such as **1** and **6** prepared with very high levels of porogen possess a pore size distribution that cannot be fully characterized by N_2 sorption experiments alone. The presence of a significant macropore population (see later) requires additional data, in the present work, from Hg intrusion experiments. The corresponding Hg intrusion volumes for all resins are shown in parentheses in Table 1, and the data for resins **1** and **6** are shown as open points in Figure 3. In the case of propyl acetate as the porogen the additional datum point leads to a good linear relationship between the pore volume and the TRIM concentration across the whole range studied, with no collapse of the pore structure (on drying) obvious down to 20 wt % TRIM. However, with butyl acetate as the porogen the Hg intrusion derived pore volume is even less than that deduced from the N_2 sorption data and tends to confirm that the pore structure is partially collapsed in this case (resin **6**), with the major shrinkage occurring on drying, rather during pore volume measurement.

The BET theory C values[34] for nearly all the resins examined are >100, e.g., for resin **5** it is ∼245. Such high values (together with the high Barret, Joyner, and Halenda (BJH)[35] adsorption volume at 1 nm; see Figures 4 and 5 and later discussion) indicate a very strong attraction between the N_2 molecules and the pore surface and are usually interpreted as indicative of a significant population of micropores. Consequently, some of the resins were subjected to careful micropore analysis via N_2 sorption. Using the Dubinin−Astakhov approach,[36] resin **3**, which has one of the highest BET surface areas (A = 557 m^2 g^{-1}; C = 116), displayed a maximum in its pore size distribution at 0.8 nm and a micropore surface area of 367 m^2 g^{-1}. Similarly, resin **9** (BET, A = 530 m^2 g^{-1}; C = 158) yielded a micropore surface area of 410 m^2 g^{-1} with a similar maximum in the pore size distribution plot. Because of the very time-consuming procedure needed for the full micropore characterization, none of the other resins were subjected to this analysis. However, since the remaining resins also displayed high BET C values and a residual low-pressure hysteresis in the N_2 sorption isotherms (Figure 1) yielding BET and BJH computed data which differ only in the detail, it seems very likely that all the resins possess a significant population of micropores. In interpreting the BET surface area data, it is important therefore to appreciate the underlying high micropore surface area contribution.

Hysteresis Effect in the N_2 Sorption Isotherms of TRIM Resins Employing Butyl Acetate as Porogen. Flodin and co-workers[7−9,11,12] noted that in the BJH pore size distribution curves for TRIM polymers prepared in solution and suspension there is always at least one sharp maximum at ∼2 nm. For example,[8] a polymer prepared in ethyl acetate yielded three maxima between ∼2 and 4 nm, and it seemed that the pore size distribution curves for pore radii below 5 nm (determined from N_2 sorption data) were independent of the porogen used in the study, whereas for radii above 5 nm, probed via Hg intrusion, a clear dependence was observed.[7−9] It is not clear in these papers, however, whether the pore size distributions (from N_2 sorption data) were computed from the adsorption or desorption branches of the isotherms. For our resins (**1**−**5**) prepared in suspension, similar distributions are observed (e.g., Figure 4 in the case of butyl acetate as the porogen) with a common maximum ∼2 nm. However, this is the case only if the BJH pore size distributions are calculated from the desorption branch of the isotherm.

Although in the past it was common to calculate pore size distributions from either the adsorption or desorption branches of the N_2 isotherm, it is now well accepted that the desorption process can be complicated by percolation problems.[25,37] The steep region commonly seen in the hysteresis loop is almost independent of the nature of adsorbent but depends mainly on the nature of adsorbing gas. For example, in the case of N_2 at 77 K the steep fall in the desorption branch appears at p/p_0 ∼ 0.42. Applying the BJH theory to such data always yields a sharp often large maximum in the pore size distribution curve ∼2 nm. For resins displaying a very large hysteresis effect, this can lead to the erroneous conclusion that a very narrow pore size distribution is present. It is important therefore that when isotherms display a hysteresis loop of this type, porosity data should be calculated from the adsorption branch only. The effect is seen very dramatically here with resins **1**−**5**; the plots in Figure 4 show the BJH pore size distribution curves calculated from the desorption branches of the N_2 isotherm with apparently sharp maxima ∼2 nm. In complete contrast, the plots in Figure 5 show the corresponding curves calculated from the adsorption branches. The same broad background distributions are apparent, covering more than 2 orders of magnitude; however, the sharp and large maximum ∼2 nm is now absent from all curves.

In interpreting the data in Figure 5 and Table 1, it is perhaps most instructive not only to consider the model dependent computed outputs from the isotherms but also to take account of the isotherm shapes, and

especially the hysteresis components. First, it is clear that the sharp maxima ~2 nm seen in the data in Figure 4 do arise from the sharp falls in the desorption branches of the isotherm indicated by the dotted lines in Figure 1. In the case of resin **5** employing 67 wt % TRIM, this is the only significant feature in the pore size distribution curve and erroneously indicates a very narrow pore size distribution. In fact, this feature arises and indeed dominates the output from the model, because of the depth and steepness of the step in the desorption branch.

A significant feature of the BJH pore size distribution curves computed from the adsorption branches of the isotherms (Figure 5) is their breadth and the steady growth in pore volume toward lower pore radii, such that for pores ~1 nm (the limit of the calculation) the pore volume of all samples is very significant. The small but sharp maximum ~1 nm seems real, and the curves suggest significant pore volume in pores below ~1 nm. As stated earlier, micropore analysis of resin **3** confirmed the presence of a second maximum in the pore size distribution ~0.8 nm.

This result was also substantiated by the application of a density functional theory approach.[38] Thus, it appears that there is a small maximum ~0.7−0.8 nm in the pore size distribution, followed by a steep rise to a second maximum ~1 nm followed thereafter by a broad rather featureless distribution through the mesopore range and into the macroporous regime. Indeed, this picture is not unreasonable on the basis of the likely mechanism of formation of the porous network.[26−28]

In the case of resins **1** and **2** prepared with the lower concentrations of TRIM, i.e., high porogen content, significant macroporosity (>50 nm) is apparent (Figure 5). At the upper limit of the N_2 sorption experiment, $p/p_0 = 1$, bulk condensation of N_2 gas would occur, and hence the isotherm obtained is "incomplete", leading to type H3 hysteresis loops[39] (Figure 1). Resin **2** employing 33 wt % TRIM shows a significant and broad maximum in its pore volume ~30 nm and is consistent with the large level of porogen present in the polymerizing mixture. This feature was also confirmed with mercury intrusion data (not shown here). Resin **1** was prepared with an even higher level of porogen, and the trend in growth of pore volume at large pore diameters with higher levels of porogen would be expected to have been maintained.[7] In fact, the distribution curve for this resin is very flat across a very broad pore size range (3 orders of magnitude), and around the mesopore/macropore boundary the curve falls well below that of resin **2**. This is almost certainly as a result of the collapse of the porous structure on drying because of the mechanical weakness (low TRIM content) of this species and has been referred to earlier with respect to total pore volume (Figure 3). In the case of resin **1** mercury porosimetry indicated the presence of some pores up to ~1 μm in diameter.

A significant change in pore structure arises with resin **3** (50 wt % TRIM) (Figure 5). First of all, the N_2 sorption isotherm is complete and is of type IV[25,30] with a type H2 hysteresis loop.[39] Almost no macropores are present, and this is confirmed with the Hg porosimetry data (not shown here). The incremental pore volume rises steadily for pores sizes ~60 to 1 nm, covering ~2 orders of magnitude. This trend is continued with resin **4** prepared with 60 wt % TRIM, the overall pore volume is reduced relative to that in resin **3** as a result of the lower porogen content, and there is little pore volume in pores above ~10 nm. Perhaps not surprisingly therefore the hysteresis loop for resin **4** is larger.

In idealized porous matrices with good pore connectivity a small hysteresis loop is often associated with a narrow pore size distribution and a large hysteresis loop with a broad distribution. With resins **3** and **4** this relationship is reversed and almost certainly arises from pore connectivity factors. Hysteresis loops can be described by percolation theory, and information on the connectivity of a porous network can be derived. Seaton et al.[40−42] have proposed a general method for the characterization of pore connectivity in terms of two parameters: a mean coordination number, Z, and a pore network size, L. However, the theory is only applicable to type H2 and within limits to type H3 hysteresis behavior and not to the type H4 displayed by resin **5**. Consequently, pore connectivity in resins **3**−**5** will be discussed only in qualitative terms. Simplistically, poor or low pore connectivity would lead to large hysteresis effects and very high connectivity to low hysteresis. As the level of TRIM employed in synthesizing resins **3**−**5** increases, the total pore volume falls (Table 1) since the level of porogen falls the complexity and density of the cross-linked polymer network formed rise. The probability therefore that two adjacent pores will be well connected to each other will therefore fall. In the limit of a very high TRIM concentration some completely isolated (closed) pores could well be generated. These trends are clear in comparing the isotherms for resins **3**−**5** where the size of the hysteresis loop increases in going from **3** to **4**, and the initial gradient of the desorption branch in **5** is almost zero. In the latter case therefore desorption is almost completely suppressed as a result of very low pore connectivity until the critical value of p/p_0 is reached when the backlog of retained N_2 desorbs relatively quickly. Resin **5** therefore, prepared from the highest level of TRIM, is characterized by a high proportion of micropores and small mesopores rather poorly interconnected, with relatively few mesopores in the 5−50 nm range.

Effect of Porogen Type on Porosity of TRIM Resins. The characteristics of TRIM resins prepared using various levels of propyl acetate as porogen are similar to those prepared using butyl acetate. The solubility parameter, δ, for the hompolymer of TRIM was determined from swelling experiments by Flodin et al.[8] and shown to be ~18.2 $MPa^{0.5}$. The solubility parameter[43] for propyl acetate (~18.0 $MPa^{0.5}$) is closer to this value than is that for butyl acetate (~17.4 $MPa^{0.5}$) so that propyl acetate is in effect a thermodynamically better "solvent" for the polymer of TRIM than is butyl acetate. Consequently, for comparable polymerization compositions, phase separation of the polymer network will be delayed somewhat in propyl acetate relative to that in butyl acetate. Less residual monomer will be available for consolidation of microgel particles and in-filling of pores,[27] and so overall the pore size distribution would be expected to shift toward smaller pores. A corollary of this is that to produce comparable pore size distributions a larger proportion of the propyl acetate porogen is required. To some extent therefore this explains the relative position of the BET surface area curves in Figure 2 for TRIM resins prepared with these two porogens. However, this is a rather naive rationalization since N_2 sorption BET surface area data are only a crude representation of pore structure, and

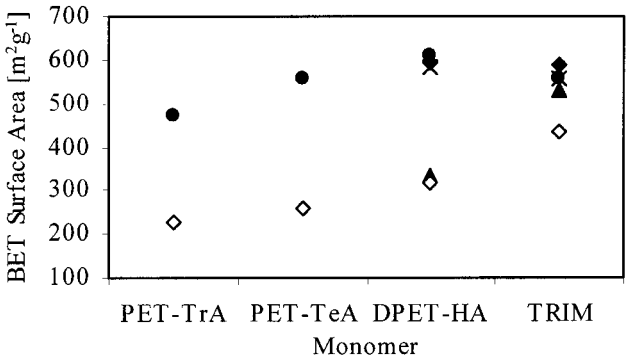

Figure 6. N_2 sorption BET surface area of resins **3** and **9**−**21**; monomer concentration = 50 wt %; porogen solubility parameter, δ [MPa$^{0.5}$]: ●, butyl acetate, 17.4; ◆, isobutyl acetate, 17.0; ×, ethyl isobutyrate, 16.2; ▲, propyl acetate, 18.0; ◇, xylene, 18.0.

the solubility parameter is a one-dimensional parameter providing only a limited understanding of the interaction between solvent and polymer. The limitation is highlighted in the case of xylene used as the porogen with 50 wt % TRIM where the resin formed (**12**) has a N_2 BET surface area of 436 m^2 g^{-1} whereas propyl acetate as porogen with 50 wt % TRIM yields resin **(9)** with a surface area of 530 m^2 g^{-1} despite both porogens having the same solubility parameter (18.0 MPa$^{0.5}$).

Effect of Porogen Type on Porosity of Multifunctional (Meth)acrylate Resins. To generate a more comprehensive set of data, a range of resins were prepared from conveniently commercially available multifunctional (meth)acrylates at 50 wt % in the porogens butyl acetate, isobutyl acetate, ethyl isobutyrate, propyl acetate, and xylene. Table 1 shows the compositional data. N_2 sorption isotherms were generated and relevant porosity data computed. Figure 6 shows a correlation of the BET surface area data. The order of the polymers on the *x*-axis has been chosen arbitrarily according to the trend in the values of the BET surface areas in the case of the porogens xylene and butyl acetate. The resins derived from the monomers PETrA, PETeA, and DPEHA lie systematically in the order of increasing multifunctionality, i.e., acrylate content. Increasing surface area (for both xylene and butyl acetate derived resins) with increasing acrylate content is superficially consistent with increasing levels of cross-linking.

Resins **13**, **15**, and **17** produced using butyl acetate as porogen show similar characteristics to resin **3** prepared with 50 wt % TRIM and butyl acetate, i.e., a broad pore size distribution from micropores through the mesoporous range with a low but positive macropore fraction. The isotherm shapes are also similar to that of resin **3** with, however, the hysteresis loop increasing in the series PETrA, PETeA, DPEHA. Considering the likely influence of this change on pore connectivity, the introduction of higher levels of polymerizable moieties (within a fixed weight percent of monomer) is likely to generate more dense polymer networks, leading to a slightly narrowed pore size distribution but also to a lower pore connectivity (i.e., in effect equivalent to increasing the weight percent of TRIM). The similarity between resins **13**, **15**, and **17** and resin **3** is perhaps not surprising bearing in mind the structural similarity between the monomers from which these are derived.

Shifting to xylene as the porogen does however give rise to a difference. The isotherm shapes and pore size distributions for resins **14**, **16**, and **21** resemble those of TRIM resins **1** and **2**, with a significant content of macropores. However, the isotherm for TRIM resin **12** is similar to that of TRIM resin **3**, with very little macroporosity. The molecular structural similarity of the multifunctional acrylate monomers with TRIM, and the resulting porosity in resins derived therefrom, thus breaks down when xylene is the porogen.

For the two monomers leading to the highest BET surface area resins (i.e., DPEHA and TRIM) several other porogens were investigated these being chosen to have solubility parameters still in the range ∼16−18 MPa$^{0.5}$. The data in Figure 6 show that there is little difference in the BET surface area of resins derived using butyl acetate, isobutyl acetate, and ethyl isobutyrate as porogen despite, for example, the solubility parameter for the latter (16.2 MPa$^{0.5}$) displaying the largest difference from that of the TRIM homopolymer than any of the porogens examined. With the TRIM resins the BET surface area falls when propyl acetate replaces butyl acetate as the porogen and falls even more when xylene is employed despite these two porogens having the same solubility parameter, which is also very similar to that of the homopolymer of TRIM. In the case of resins **18** and **21** derived from DPEHA and propyl acetate and xylene, respectively, there is good consistency between the BET surface areas (Figure 6) and the common solubility parameter (18.0 MPa$^{0.5}$). However, the isotherm of the xylene resin **21** is very similar to that of resin **1** (Figure 1) showing significant macroporosity, whereas that of the propyl acetate resin **18** is very like that of resin **5** (Figure 1) being dominated by small mesopores and micropores. The coincidence of BET surface area data is therefore fortuitous and misleading and clearly use of simple solubility parameter data is not adequate when trying to predict the finer pore structure.

Use of Three-Dimensional Cohesion Parameters, δ_t, in Correlating Resin Pore Structure. Not surprisingly, factors such as dispersion forces, polar forces, and hydrogen bonding, and their influence in controlling resin pore structure via use of porogens, cannot be summarized in terms of a single simple solubility parameter. The most commonly used one-dimensional Hildebrand parameter, based on enthalpies of vaporization,[43] is too simplistic. A much better correlation may be provided by a three-dimensional cohesion parameter, δ_t,[22−24] which considers the contributions from dispersive, δ_d, dipolar, δ_p, and hydrogen bonding, δ_h, interactions. In a three-dimensional diagram the porogen and polymer can be represented by two points, and the porogen−polymer affinity can be described by the distance d_0 between these two points.[22]

$$\delta_t^2 = \delta_d^2 + \delta_p^2 + \delta_h^2$$

$$d_0^2 = 4(\delta_{d1} - \delta_{d2})^2 + (\delta_{p1} - \delta_{p2})^2 + (\delta_{h1} - \delta_{h2})^2$$

The indices 1 and 2 represent the porogen and polymer, respectively. Although many of these cohesion parameters, such as the Hansen or Hoy parameters,[44] are tabulated in the literature, we were faced with the rather common problem that data for not all porogens, and none of the polymers are available.

Therefore, an attempt was made to apply a group contribution method according to Hoftyzer−Van Krevelen and Hoy.[43,45] Since all polymers are homopolymers

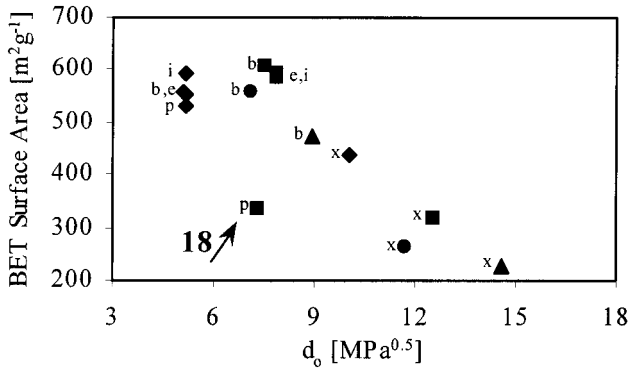

Figure 7. N_2 sorption BET surface area vs polymer−porogen affinity parameter d_0 of resins **3** and **9**−**21**: ◆, TRIM; ■, DPEHA; ▲, PETrA; ●, PETeA. Porogens indicated by letters: b = butyl acetate, e = ethyl isobutyrate, i = isobutyl acetate, p = propyl acetate, x = xylene.

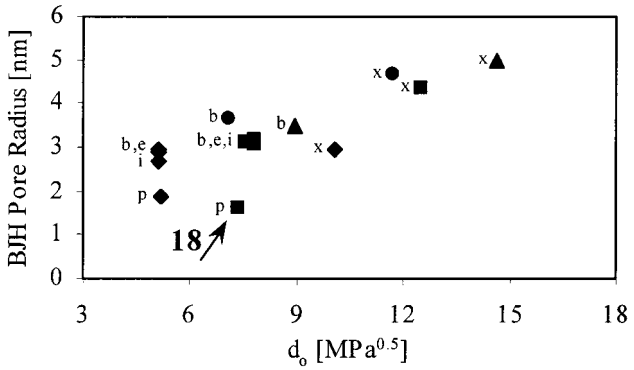

Figure 8. N_2 sorption BJH pore radius vs polymer−porogen affinity parameter d_0 of resins **3** and **9**−**21**: ◆, TRIM; ■, DPEHA; ▲, PETrA; ●, PETeA. Porogens indicated by letters: b = butyl acetate, e = ethyl isobutyrate, i = isobutyl acetate, p = propyl acetate, x = xylene.

of multifunctional monomers exhibiting a significant double-bond content after polymerization, the remaining free (meth)acrylate groups were also to be considered in the calculations. In the case of contributions from *n* components (e.g., with xylene), the average cohesion parameters were calculated according to the following equation[23]

$$\bar{\delta}_i = \phi_1\delta_{1i} + \phi_2\delta_{2i} + ... + \phi_n\delta_{ni}$$

whereas ϕ represents the volume fractions, and the index *i*, the type of dispersive interaction (d, p, and h). Both methods (Hoftyzer−Van Krevelen and Hoy) are of the same order of accuracy, and it has been suggested that these should be averaged.[45] The calculated polymer−porogen affinity parameters d_0 were correlated with the BET surface area and the BJH average pore radius, respectively. Both methods used alone yielded similar relationships, but the scattering of data points was significantly reduced using average values from both methods.

Data for the BET surface area and the BJH average pore radius for all resins prepared with 50 wt % monomer are plotted against the polymer−porogen affinity parameter, d_0, in Figures 7 and 8, respectively. A similar plot against pore volume led to a scatter of points showing no trends. However, nearly all the resins in question, though having a major fraction of pores in the meso- and microporous range, did have some macroporosity, the volume of which is not accounted for in N_2 sorption. In addition, the compressibility of meso- and micropores during Hg intrusion also introduces uncertainty in pore volume measurements. The lack of correlation of d_0 with (apparent) total pore volume was therefore not regarded as a serious deficiency. The correlation between BET surface area and d_0 (Figure 7) overall shows an inverse proportionality, while that with BJH pore radius is a directly proportional one. The literature[22] defines good solvents with $d_0 < 10.0$, intermediate solvents with $10.0 < d_0 < 12.7$, and bad solvents with $d_0 > 12.7$. This seems appropriate here since empirically the ester porogens would be expected to be good solvents for the polymers involved because of the structural similarly with the monomer segments (Table 1). The same argument is true in categorizing xylene by its d_0 values as a poor solvent. The correlation shown in Figure 7 is significantly superior to that provided by consideration of the one-dimensional solubility parameter, δ, alone. The difference between the two porogens, propyl acetate ($\delta = 18.0$; $\delta_d = 15.1$; $\delta_p = 6.5$; $\delta_h = 9.8$) and xylene ($\delta = 18.0$; $\delta_d = 17.6$; $\delta_p = 4.1$; $\delta_h = 1.4$), is now seen clearly. (δ represents the experimentally determined Hildebrand solubility parameter[43] and cannot be derived from the three parameters δ_d, δ_p, and δ_h, which were calculated according to the group contribution methods.[43,45])

The model also predicts the behavior of PETrA, the monomer that contains the highest number of free −OH groups per ester function. This monomer would be expected to yield homopolymer that phase separates earlier in polymerizations than the others because of reduced compatibility with the porogens. This in turn would be expected to lead on average to larger pores (Figure 8) and hence lower surface areas[27] (Figure 7). Monomer, DPEHA, with a lower −OH group content per ester group would be expected on average to yield smaller pores than PETrA under comparable conditions with these porogens, and this is the case in practice. The parameter d_0 seems slightly underestimated in the case of the interactions involving PETeA and is generally similar to the values for DPEHA.

The differences between resins derived from PETeA and TRIM also seem to be rationalized. These are structurally very similar monomers (and polymers), and the higher functionality of PETeA vs TRIM (for equal weight percent) could lead to the expectation that the derived resins would on average yield smaller or similar pore sizes and consequently higher surface areas. However, the reverse behavior is found in practice, in accordance with the higher d_0 values for the resins obtained from PETeA. According to the group contribution methods, it seems that the PETeA resins show higher δ_d and δ_h, but especially higher δ_p values causing the larger d_0 values compared to those of TRIM.

The data for resin **18** lie significantly outside the correlations displayed by the other resins, and although the model applied seems erroneous, there seems no reason propyl acetate should give rise to this anomaly; i.e., the d_0 value seems fine. This suggests therefore that the problem resides in the porosity data and the resin structure. Examination of N_2 sorption isotherm for resin **18** shows that it has a very pronounced type H4 hystersis loop. The morphology corresponds closely therefore to that of resin **5**. Phase separation of polymer probably occurs rather late in the polymerization with the generation of small pores, but these must have rather poor connectivity as well. In addition, this resin

has an extremely low pore volume (Table 1) as does resin **5**, far lower than the other resins in this study. In the case of resin **5** this arises from the very low level of porogen present in the polymerization, but this explanation cannot be invoked for resin **18**. It is shown in Figure 2 that the porous structure of TRIM resins is dependent on the concentration of the monomer mixture over a wide range, whereas the maximum surface area appears to be rather flat. It is very likely that a similar relationship occurs for the other monomers, but the position of the maximum and the steepness of the curve could be significantly different. The choice of a monomer concentration of 50 wt % was arbitrary but has apparently led to an almost gel-type morphology for resin **18**; i.e., its porous morphology is not sufficiently developed to correlate well with the other data points. It is worth noting that resin **18** is the only one in Figures 7 and 8, exhibiting a clear type I isotherm and type H4 hysteresis loop. A weak point is certainly that the applied models for the calculation of the porogen−polymer affinity parameter d_0 do not take into account the monomer concentration, but a good correlation can be found for all resins as long as a sufficient number of mesopores or even macropores are being developed leading to type IV and type II isotherm shapes, respectively.

Overall, therefore, the use of the three-dimensional cohesion parameter, δ_t, to correlate pore structure with polymer−porogen interactions even in the range where only subtle changes are involved seems relatively successful and certainly superior to the commonly used correlation involving the one-dimensional solubility parameter.

Conclusions

The effect of TRIM concentration on the porous structure of resins prepared with butyl acetate as porogen is complex. The maximum BET surface area is seen ∼40 wt % TRIM and the maximum pore volume ∼30 wt % TRIM. At the lowest TRIM level ∼20 wt % the resin structure tends to collapse on drying. All resins display significant microporosity, and the species derived from 33 wt % TRIM is also significantly macroporous. As the level of TRIM employed is increased to 67 wt %, macroporosity is lost and the balance between mesopore and micropores gradually shifts toward small mesopores and micropores, such that with 67 wt % TRIM few pores exist >5 nm. At same time, however, the connectivity of pores becomes increasingly impaired, with the 67 wt % TRIM resin showing a prolonged delay in any desorption of N_2 during isotherm measurement. Computation of porosity data must be made from the adsorption branch of the N_2 isotherm. Significant hysteresis loops in the latter are translated into erroneous pore size distribution curves if calculations are based on the desorption branch of the isotherm. In particular, apparently very narrow pore size distributions can be derived but these are totally artifactual. The variety in pore structures offered by manipulation of the TRIM−porogen combination is broader than indicated simply by for example N_2 BET surface area data and offers considerable choice in terms of potential application.

The synthesis and porosity characterization of a much wider range of resins from a number of multifunctional (meth)acrylates and porogens has allowed a more extensive correlation of porous morphology with polymer molecular structure and porogen type. Rationalization of porosity data with the one-dimensional Hildebrand solubility parameter, δ, for polymers and porogens is useful but fails completely in some circumstances. A much more comprehensive correlation is obtained using three-dimensional cohesion parameters, δ_t, and in particular by calculating porogen−polymer affinity in terms of d_0, the distance between the porogen and polymer δ_t values in three-dimensional space. N_2 sorption BET computed surface areas of resins show an inverse linear relationship with d_0, while BJH average pore radii show a linear relationship. While total pore volume shows no clear correlation, this probably arises, because neither N_2 sorption nor Hg intrusion porosimetry alone is able to evaluate pore volume accurately for resins with both significant micropore and macropore populations.

References and Notes

(1) *Resin Chromatography Products*, Issue No. 2; Polymer Laboratories Limited: Essex Road, Church Stretton, Shropshire, SY6 6AX, UK, 2001/2002.
(2) *Combinatorial Peptide and Nonpeptide Libraries*; Jung, G., Ed.; VCH Pubs.: Weinheim, Germany, 1996.
(3) *A Practical Guide to Combinatorial Chemistry*; Czarnik, A. W., DeWitt, S. H., Eds.; American Chemical Society: Washington, DC, 1997.
(4) Ley, S. V.; Baxendale, J. R.; Bream, R. N.; Jackson, P. S.; Leach, A. G.; Taylor, S. J. *J. Chem. Soc., Perkin Trans. 1* **2000**, 1931.
(5) *Ion Exchangers*; Dorfner, K., de Gruyter, W., Eds.; Berlin, Germany, 1991.
(6) *Affinity Chromatography—A Practical Approach*; Dean, P. D. G., Johnson, W. S., Middle, F. A., Eds.; IRL Press: Oxford, UK, 1985.
(7) Rosenberg, J.-E.; Flodin, P. *Macromolecules* **1986**, *19*, 1543.
(8) Rosenberg, J.-E.; Flodin, P. *Macromolecules* **1987**, *20*, 1518.
(9) Rosenberg, J.-E.; Flodin, P. *Macromolecules* **1987**, *20*, 1522.
(10) Rosenberg, J.-E.; Flodin, P. *Macromolecules* **1988**, *21*, 2041.
(11) Schmid, A.; Kulin, L. I.; Flodin, P. *Makromol. Chem.* **1991**, *192*, 1223.
(12) Schmid, A.; Flodin, P. *Makromol. Chem.* **1992**, *193*, 1579.
(13) Viklund, C.; Ponten, E.; Glad, B.; Irgum, K.; Horstedt, P.; Svec, F. *Chem. Mater.* **1997**, *9*, 463.
(14) Kolarz, B. N.; Wojaczynska, M.; Trochimczuk, A. W. *Makromol. Chem.* **1993**, *194*, 1299.
(15) Kolarz, B. N.; Wojaczynska, M.; Bryjak, J.; Laborzewski, J. *Makromol. Rep.* **1993**, *A30* (Suppl. 3, 4), 201.
(16) Kolarz, B. N.; Wojsczynska, M.; Bryjak, J.; Lobarzewski, J.; Pawlow, B. *J. Appl. Polym. Sci.* **1995**, *58*, 1317.
(17) Kolarz, B. N.; Wojsczynska, M. *Polymer* **1998**, *39*, 69.
(18) Kolarz, B. N.; Jermakowicz-Bartkowiak, D.; Trochimczuk, A. *Eur. Polym. J.* **1998**, *34*, 1191.
(19) Kannurpatti, A. R.; Anseth, J. W.; Bowman, C. N. *Polymer* **1998**, *39*, 2507.
(20) Cooper, A. I.; Wood, C. D.; Holmes, A. B. *Ind. Eng. Chem. Res.* **2000**, *39*, 4741.
(21) Wood, C. D.; Cooper, A. I. *Macromolecules* **2001**, *34*, 5.
(22) Rabelo, D.; Coutinho, F. M. B. *Polym. Bull.* **1994**, *33*, 479.
(23) Rabelo, D.; Coutinho, F. M. B. *Polym. Bull.* **1994**, *33*, 487.
(24) Rabelo, D.; Coutinho, F. M. B. *Polym. Bull.* **1994**, *33*, 493.
(25) Sing, K. S. W.; Everett, D. H.; Haul, R. A. W.; Moscou, L.; Pierotti, R. A.; Rouquérol, J.; Siemieniewska, T. *Pure Appl. Chem.* **1985**, *57*, 603.
(26) Albright, R. L. *React. Polym.* **1986**, *4*, 155.
(27) Sherrington, D. C. *Chem. Commun.* **1998**, *21*, 2275.
(28) Okay, O. *Prog. Polym. Sci.* **2000**, *25*, 711.
(29) Hubbard, K. L.; Finch, J. A.; Darling, G. D. *React. Funct. Polym.* **1999**, *40*, 61 and earlier references therein.
(30) *Analytical Methods in Fine Particle Technology*; Webb, P. A., Orr, C., Eds.; Micromeritics Instrument Corp.: Norcross, GA, 1997; p 55.
(31) See ref 26, p 61.
(32) Howdle, S. M.; Jerabek, K.; Leocarbo, V.; Marr, P. C.; Sherrington, D. C. *Polym. Commun.* **2000**, *41*, 7273.
(33) Hradil, J.; Svec, F. *Angew. Makromol. Chem.* **1985**, *130*, 81.
(34) See ref 28, p 62.

(35) See ref 28, p 80.
(36) See ref 28, p 73.
(37) Lee, C. K.; Chiang, A. S. T.; Tsay, C. S. *Key Eng. Mater.* **1996**, *115*, 21.
(38) See ref 28, p 81.
(39) See ref 34, p 27.
(40) Seaton, N. A. *Chem. Eng. Sci.* **1991**, *46*, 1895.
(41) Liu, H.; Zhang, L.; Seaton, N. A. *Chem. Eng. Sci.* **1992**, *47*, 4393.
(42) Liu, H.; Seaton, N. A. *Chem. Eng. Sci.* **1994**, *49*, 1869.
(43) Grulke, E. A. In *Polymer Handbook*, 4th ed.; Brandrup, J., Immergut E. H., Grulke, E. A., Eds.; Wiley-Interscience: New York, 1999; Chapter VII, p 675.
(44) Barton A. F. M. In *CRC Handbook of Solubility Parameters and Other Cohesion Parameters*, 2nd ed.; CRC Press: Boca Raton, FL, 1991.
(45) Van Krevelen. D. W. In *Properties of Polymers*, 3rd ed.; Elsevier: New York, 1990; Chapter 7, p 189.

MA0110958